



Preparation, characterization and dielectric properties of sodium alginate/titanium dioxide composite membranes

G. T. Padma¹ · T. Subba Rao¹ · K. Chandra Babu Naidu²

© Springer Nature Switzerland AG 2018

Abstract

Sodium alginate/titanium dioxide solid polymer composite membranes were prepared by solution casting method. The electrical, optical and thermal properties of these composite membranes are in great demand for advanced electronic device applications. The present study is aimed at the preparation of dioxide membranes to enhance the conductivity of sodium alginate. The diffraction pattern confirmed the change of sodium alginate polymer matrix structure from amorphous to polycrystalline upon dispersing TiO₂ powder particles into sodium alginate solution. The surface morphology also evidenced the non-crystalline and polycrystalline (containing grains and grain boundaries) nature of formed films. The infrared spectra showed the presence of various functional groups such as –OH, C=O, O–H, C–H and Na–O. The differential scanning calorimeter (DSC) investigation revealed the existence of exothermic/endothemic peaks, melting and crystallization temperatures. Furthermore, the weight loss of all the films was described as a function of temperature. The dielectric properties highlighted the 5 wt% of TiO₂ dispersed in the sodium alginate solution due to its high dielectric constant (ϵ'), dielectric loss (ϵ'') and ac-electrical conductivity (σ_{ac}).

Keywords Amorphous materials · Polymer composites · Microstructure · Electrical properties · X-ray techniques

1 Introduction

Polymer composite membranes continue to receive tremendous attention for their potential advanced material applications [1]. Polymer composite membranes are the polymer membranes in which small amount of powder particles are dispersed. The physical, chemical, and electrostatic interactions between the polymer and filler result in improvements of electrical, optical, mechanical, thermal properties of polymer membranes [1–4]. These are needed to meet the demand in emerging technological applications for such advanced materials. More recently, the significant development occurred in the area of flexible electronic devices.

Sodium alginate (SA) is an environmentally safe, inexpensive, nontoxic, weak acidic, anionic, and linear

chained natural polysaccharide material [1]. Recently, the SA acquired more significance because of its diverse properties as well as gel forming capability with metal oxides [1]. Thus, the usage of SA revealed distinct applications in controlled drug delivery, dehydration of organic solvents, removal of metal ions from aqueous solutions, textile industries, food industries etc., [1]. In addition, the SA based polymeric specimen exhibited high ϵ' which in turn responsible for potential applications in actuators, artificial muscles, and charge stored capacitors [3]. The polymers containing high ϵ' can also adopt high ϵ'' . Therefore, it promotes the electrical conductivity to larger extent. Moreover, the polymer composite membranes possessing high σ_{ac} value showed extensive applications in molecular electronics [2]. In order to increase the electrical conductivity and dielectric constant in polymers, one has

✉ T. Subba Rao, thotsubbarao6@gmail.com; ✉ K. Chandra Babu Naidu, chandrababu954@gmail.com | ¹Department of Physics, Sri Krishnadevaraya University, Anantapuramu, A.P, India. ²Department of Physics, GITAM Deemed to be University, Bangalore, Karnataka, India.

to disperse the ceramic powder particles with high dielectric constant into the polymer solution. In this concern, many scientists used to disperse the inorganic powder particles into the polymer solution such as SA and polyaniline [4–11]. Subsequently, biomedical, electronic device and environmental cleaning applications were obtained. Hence, the polymer composite membranes can be synthesized. In the literature [2] TiO_2 fillers were added to the polyaniline for further increase of dielectric constant and electrical conductivity. At this juncture, the authors got an idea to introduce the TiO_2 fillers into the SA polymer solution in order to achieve the good dielectric constant and electrical conductivity. However, in the literature very limited studies were found on SA/ TiO_2 polymer composite membranes [12–15].

2 Experimental procedure

2.1 Materials

Sodium Alginate (viscosity > 2000 CP) (SDFC, 99.4% purity) and TiO_2 (Merck, 99.2% purity) were used as the starting materials. Double distilled water was used throughout the experiment for film casting.

2.2 Membrane preparation

The polymer composite membranes of sodium alginate dispersed with TiO_2 were prepared by solution casting method. At first, 4 wt% of sodium alginate solution was prepared by continuous magnetic stirring of 4 g amount of NaAlg in 90 ml of water for 48 h. The required amount of TiO_2 (5, 10, 15 wt% based on weight of NaAlg) for each sample was first dispersed in 10 ml of distilled water under ultrasonication for 2 h at room temperature. The well dispersed TiO_2 then added to an aqueous of 4 wt% of NaAlg solution. Furthermore, it was magnetically stirred until completely dissolved in order to obtain a homogeneous NaAlg– TiO_2 viscous solution. This solution was poured into a polypropylene petri dish and left to dry at room temperature in order to obtain free standing polymer composite membranes. The thickness of NaAlg– TiO_2 films for 0, 5, 10, 15 wt% concentrations of TiO_2 were 0.12, 0.12, 0.13 and 0.13 mm respectively. These are indicated by SA, SA1, SA2 and SA3 respectively. These films were initially dried in vacuum. Further, the films were subjected for different characterization techniques like X-ray diffractometer (Bruker X-Ray Powder Diffractometer, $\text{Cu}_{\text{K}\alpha}$, $\lambda = 0.15406$ nm), Scanning Electron Microscope (Ultra 55 SEM Carl Zeiss), FT-IR spectrophotometer (IR affinity-1, Shimadzu), Differential Scanning Calorimeter (DSC 131, Setaram), Thermo gravimetric Analyzer (TGA, Linseis STA PT 1750) and LCR

HiTESTER (HIOKI 3532-50, Japan) for structural, morphological, functional group, thermal and dielectric properties respectively.

3 Results and discussion

3.1 X-ray diffraction (XRD) analysis

The diffraction patterns of all membranes along with pure TiO_2 were presented in the Fig. 1. There are no crystalline phases in the diffraction pattern of SA film. But nevertheless, a weak and broad diffraction peak at $2\theta = 14.92^\circ$ is noted for SA film. It may be generally happened owing to the instrumental error. Therefore, as a whole, it indicates the amorphous (non-crystalline) structure of sodium alginate. In the case of TiO_2 , the maximum intense peak at 27.68° confirmed its rutile crystalline phase. The miller indices (hkl) (110), (101), (200), (211), (220), (002), (310), and (301) are assigned to the diffraction angles 36.3° , 41.49° , 54.53° , 56.82° , 63° , 64° , 69.23° and 70.1° respectively. As 5, 10, 15 wt% of TiO_2 amounts are dispersed in SA matrix, there is no significant difference in diffraction angles found for SA/ TiO_2 films and pure TiO_2 . But indeed, the decrease in intensity of peaks with decrease in concentration of TiO_2 in SA films is observed. This indicates that there is no change on morphology of TiO_2 which is attributed to the

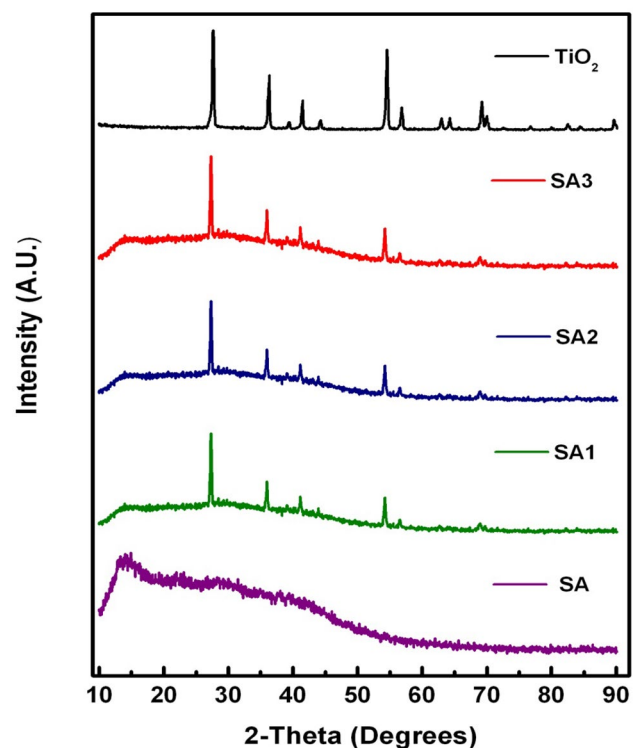


Fig. 1 XRD pattern of SA/ TiO_2 films

favorable interaction between TiO_2 and SA matrix. Hence, these results suggest successful incorporation of TiO_2 particles into sodium alginate matrix. In addition, the more clarity in the crystalline phases is found for pure TiO_2 when compared with the dispersed materials. This confirms a fact that with increase of SA content in the titanium dioxide the phase identification becomes much clear. Thus, the conversion from non-crystalline to polycrystalline formation is obviously observed.

3.2 SEM analysis

SEM photographs of the surface morphology for the NaAlg/ TiO_2 are shown in the Fig. 2. Depending on the

amount of TiO_2 present in the polymer matrix, the morphology of NaAlg/ TiO_2 composite membranes will vary and greatly influence its properties. These images show many aggregates or chunks distributed on the top surface indicating the TiO_2 particles tended to form aggregates and dispersed into NaAlg polymer matrix. From the images of pure NaAlg and NaAlg titanium dioxide composites, it was observed that the apparent roughness and whiteness (due to small particle size) increases with increase of the content of TiO_2 and its dispersion in polymer matrix. In case of the distribution of grains, the homogeneous grains were seen. But these were accommodated like cluster of grains at different spots of the polymer films. Particularly, the shape of grains was almost seemed to be like stones.

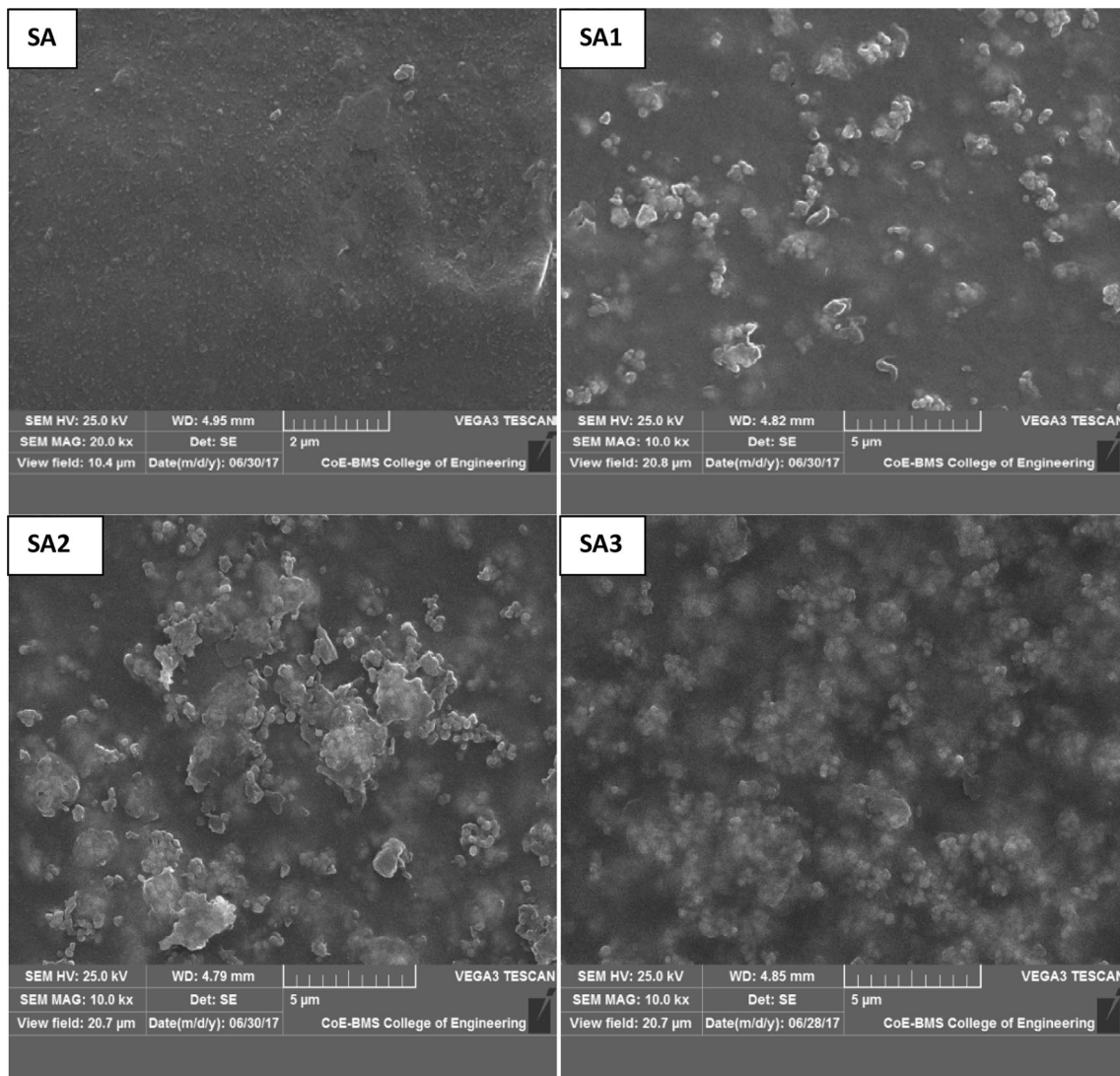


Fig. 2 SEM micrographs of SA/ TiO_2 films

3.3 FTIR analysis

FTIR analysis (Fig. 3) is used to analyze characteristic bonds. The FTIR spectrum of TiO₂ has broad absorption bands at 3371, 1596 and 1388 cm⁻¹ that are attributed to -OH, C=O vibrations respectively. In case of polymer composite membranes, in FTIR spectrum of SA membrane, the peak at 3409, and 2815–2731 cm⁻¹ are assigned to stretching vibrations of O–H [16–18] and C–H bonds [2] respectively. The strong absorption bands at 1596 and 1388 cm⁻¹ are attributed to the asymmetric stretching vibration of (C=O) carboxylate group. The peaks at 763, 702, and 609 cm⁻¹ attributed to Na–O bond in SA [2]. After the incorporation of TiO₂ into these membranes, the FTIR spectra show the systemic increase in OH absorption with increase in concentration of TiO₂. This in turn leads to increase in intensity which is determined from the interaction between TiO₂ and NaAlg.

3.4 DSC analysis

The Fig. 4 shows DSC curves of the mixed matrix membranes. It is evident that the heat flow is first decreasing with increase of temperature up to approximately 100 °C and beyond that the heat flow started to increase till 185.76 °C. The DSC curve of SA showed sharp endothermic peak at 185.76 °C and is associated to melting temperature. This peak was shifted to higher temperature region of 218.71 °C, 218.9 °C, and 219.22 °C for SA1, SA2 and SA3 respectively when sodium alginate is incorporated with titanium dioxide. This confirmed a fact that the incorporation of inorganic filler TiO₂ into sodium alginate matrix attributes to increase in the crystallization from pure SA to

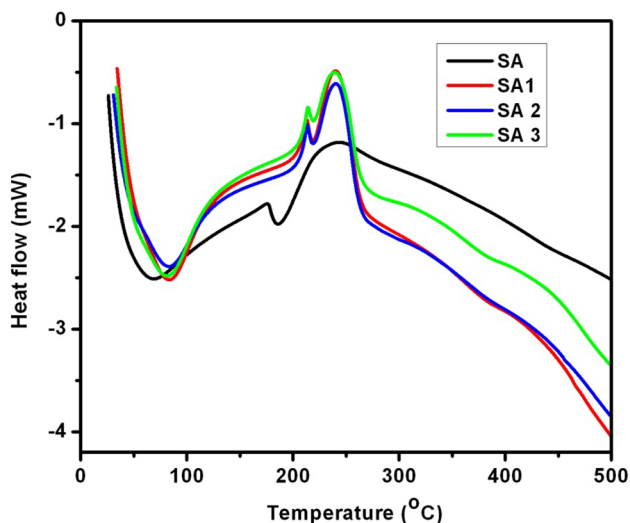


Fig. 4 Variation of heat flow versus temperature

SA3. For further increase of temperature, the heat flow is diminished beyond 260 °C which is a usual behavior.

3.5 TGA analysis

In general, TGA is used to find the thermal stability of present polymer film. With increase of temperature, the thermal degradation of polymer film is observed. It is obvious from the Fig. 5 that the weight loss was decreased with increase of temperature from room temperature to 600 °C. The weight loss is found at two different temperatures. That is, the TGA curves (Fig. 5) of pure sodium alginate and sodium alginate-TiO₂

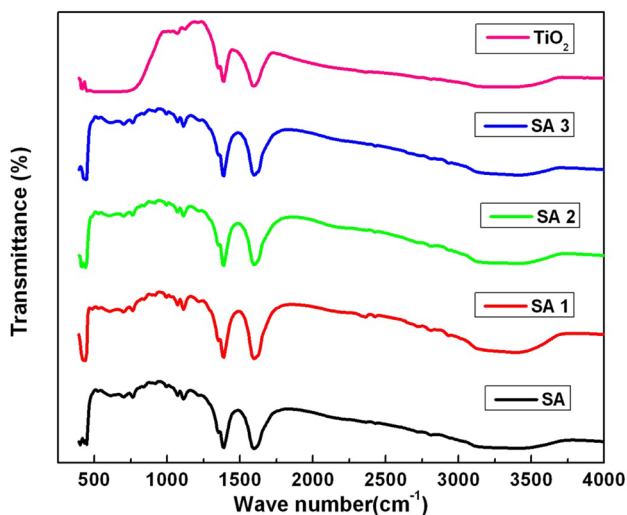


Fig. 3 FTIR spectra of SA/TiO₂ films

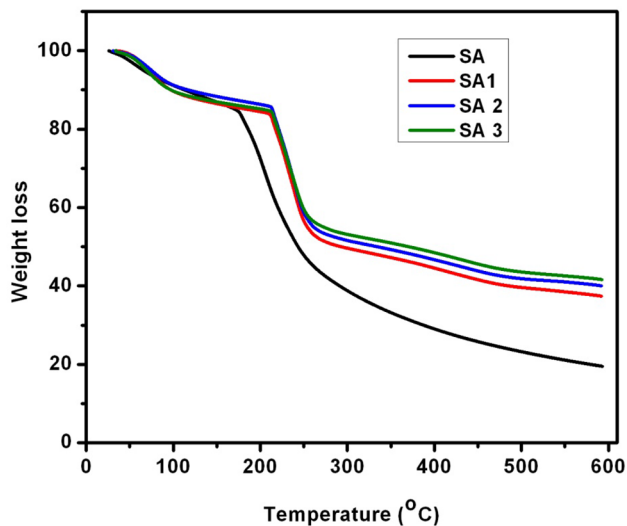


Fig. 5 Variation of weight loss versus temperature

membranes show the two-stage degradation behavior. The first stage corresponds to 10–15% weight loss from room temperature to 180 °C due to expulsion of moisture and residual solvent in sodium alginate. The major weight loss occurred above 180 °C. As concentration of TiO₂ increases, a decrease in weight loss is noted with increase in temperature. At high concentration of TiO₂, the high thermal stability is noticed. This establishes a fact that the SA1, SA2 and SA3 samples expressed almost constant trend of weight loss with increase of temperature. Therefore, it indicates the thermal stability between 250 and 600 °C.

3.6 Dielectric properties

The dielectric behaviour of polymer composite materials is a powerful technique for studying relaxation and conduction mechanisms in polymer material. Dielectric permittivity is complex quantity given by: $\epsilon^* = \epsilon' - i\epsilon''$, where ϵ' and ϵ'' are the real and imaginary parts permittivities. The real part generally is referred as dielectric constant while the imaginary part is associated to the dielectric loss. The dielectric constant is calculated by using the relation: $\epsilon' = Cd/A\epsilon_0$, where 'C' is the capacitance, 'A' is area of cross section of material, 'd' is the thickness and permittivity of free space [19]. The dielectric loss ($\epsilon'' = \epsilon' \tan\delta$) is computed using the product of dielectric constant and loss tangent [20]. Both ϵ' and ϵ'' parameters of SA, SA1, SA2, and SA3 mainly depend on two factors such as applied temperature and frequency. These are described as follows.

3.7 Temperature dependence of ϵ' and ϵ''

The variation of dielectric constant and dielectric loss with temperature at 1 MHz frequency is shown in the Fig. 6. The dielectric constant remained a constant value for all the samples up to 90 °C. Beyond this temperature, ϵ' is increased with increase of temperature. On the other hand, the dielectric loss exhibited a slow increasing trend with temperature till 80 °C. Above this temperature, a drastic increasing manner is seen. It can be attributed to the fast response of charge carriers in the membranes [21, 22]. However, it is observed that dielectric constant and dielectric loss performed the relaxation behaviour with temperature and undergone transition. This type of relaxation behavior is attributed to the accumulation of charge carriers at the grain boundary interface. Thus, the resonance takes place and further it leads to the peaking value of both dielectric constant and loss values. The dielectric behavior of the pure polymer and membranes SA2, SA3 is same (except SA1). Among all these membranes, SA1 composite membrane shows very interesting behavior in respect of dielectric properties. The highest values of dielectric constant and dielectric loss with temperature are 0.36 and 0.06 respectively for SA1.

3.8 Frequency dependence of ϵ' and ϵ''

Figure 7 shows the variations of the dielectric constant and dielectric loss with frequency for different concentrations of TiO₂ at 311 K. The dielectric constant and dielectric loss are decreased with increase in frequency. High value of dielectric constant at low frequencies is due to space charge polarization (interfacial polarization) [23]. This

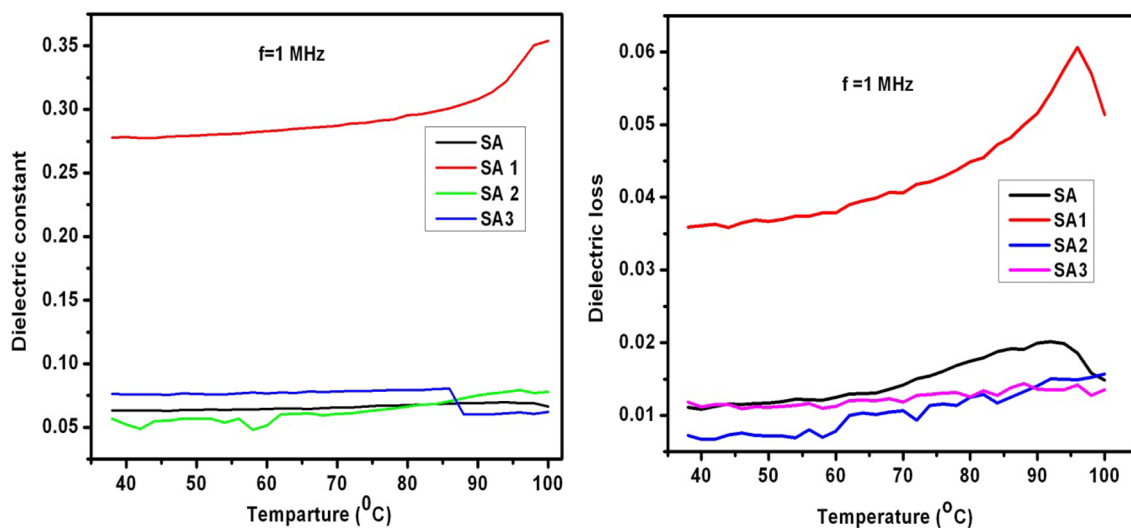


Fig. 6 Temperature dependence of ϵ' and ϵ'' of SA/TiO₂ films

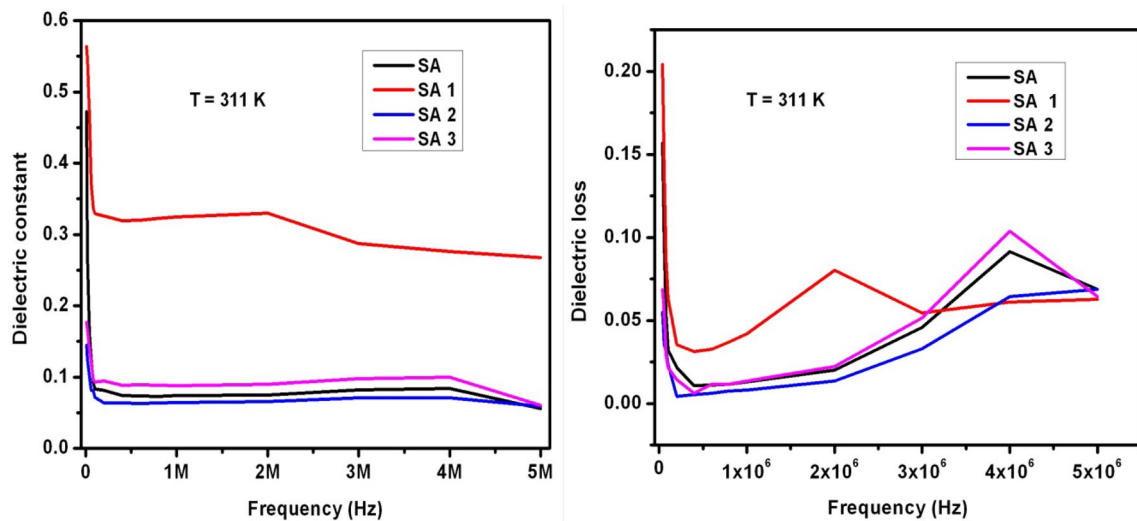


Fig. 7 Frequency dependence of ϵ' and ϵ'' of SA/TiO₂ films

value decreases which could be due to dipoles unable to follow the field variation at high frequencies. As frequency goes on increasing, the pure SA, SA2, SA3 shows similar behavior i.e. they exhibit increasing of ϵ' and ϵ'' values at particular frequency instead of usual dielectric behavior [24–26]. In general, the polycrystalline materials are composed of two segments such as grains and grain boundaries. The high value of dielectric constant and loss can be attributed to the grain boundary effect. Since, the grain boundaries are more active at lower frequencies. Further at high frequencies, the grains become more active and subsequently, the ϵ' and ϵ'' parameters will be reduced. This behavior is different for SA1 between 2 and 3 MHz. That

is, ϵ' and ϵ'' started to increase. For the further increase of frequency again the ϵ' and ϵ'' are decreased. It can be attributed to noticeable enhancement of polarization of composites. The highest values of dielectric constant and dielectric loss with frequency are 0.56 and 0.2 respectively for SA1 at 10 kHz.

3.9 Temperature and frequency dependence of AC-conductivity

The Fig. 8 shows the variation of ac-conductivity as a function of temperature and frequency. As the temperature goes on increasing, the ac-conductivity gradually

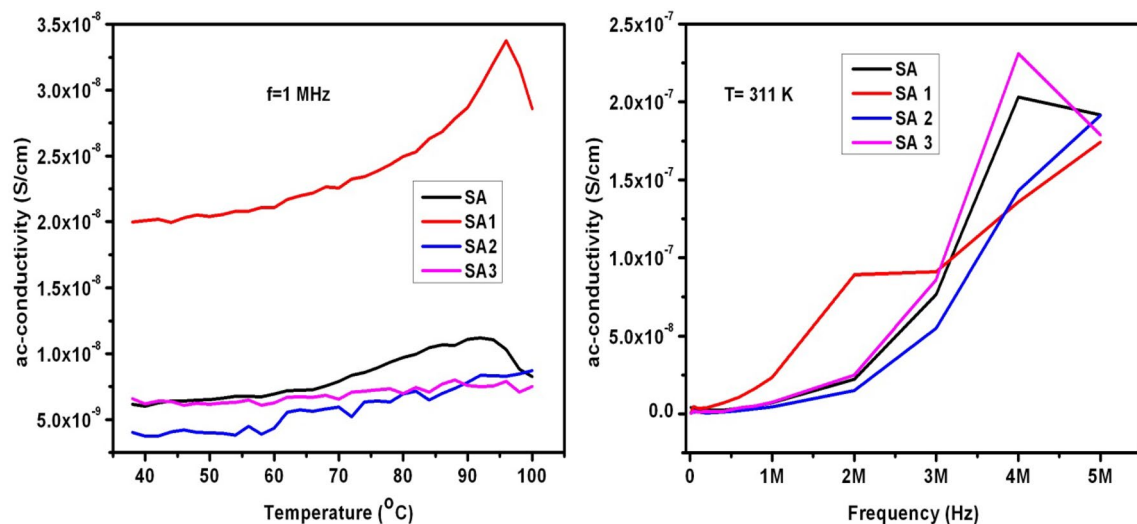


Fig. 8 Temperature and frequency dependence of ac-conductivity of SA/TiO₂ films

increases. This kind of manner may be acquired due to increase of hopping of charge carriers. That is, for the present samples, the ac-conductivity is almost constant up to 70 °C. This can be achieved as a result of the less response of charge carries for the provided temperature. In general, these polymer films will have less number of charges. For further increase of temperature, the ac-conductivity starts gradually increasing for all the materials. It normally implies that the dielectric relaxation becomes thermally activated and hence this can be governed by Arrhenius equation: $\sigma_{ac} = \sigma_0 \exp(-E_a/K_B T)$, σ_0 is pre-exponential factor, K_B is the Boltzmann's constant, E_a is the activation energy and T is the absolute temperature [23–28]. The high ac-conductivity achieved in this study is 3.3×10^{-8} S/cm at 369 K for SA1. The dielectric constant and dielectric loss are high at particular frequency. This variation in turn allows having high ac-conductivity at that particular frequency. The high ac-conductivity achieved in this study is 2.3×10^{-7} SA3 at 4 MHz. Therefore, this kind of high conducting polymer composite membranes may be expected for molecular electronics [2].

4 Conclusions

- The SA/TiO₂ polymer composite membranes were prepared by solution casting method.
- The diffraction pattern confirmed the change of sodium alginate polymer matrix structure from amorphous to polycrystalline on dispersing the TiO₂ powder particles into sodium alginate solution.
- The SEM micrographs evidenced the non-crystalline and polycrystalline nature of formed films.
- The FTIR spectra showed the existence of functional groups like –OH, C=O, O–H, C–H and Na–O.
- The DSC curve of SA showed sharp endothermic peak at 185.76° and is associated to melting temperature. This peak was shifted to higher temperature region of 218.71°, 218.9°, 219.22° for SA1, SA2 and SA3 respectively.
- The TGA analysis showed the major weight loss above 180 °C due moisture and residual solvent in sodium alginate.
- The high dielectric constant and loss observed at 5 wt% of TiO₂ dispersed in the sodium alginate solution.
- The high $\sigma_{ac} \sim 2.3 \times 10^{-7}$ noticed for SA3 at 4 MHz may be well suited for molecular electronics applications.

Acknowledgements The authors express thankful to Prof. T. Subba Rao, S. K. University, Anantapur, A.P., for helping in sample preparation.

Author's contributions The work is contributed by the all authors according to the priority given in the name section. In addition, these samples are not creating any problems to the nature or living organic matter.

Compliance with ethical standards

Conflict of interest The authors declare that we have no conflicts of interest.

References

1. Chandrakala HN, Ramaraj B, Shivakumaraiah, Siddaramaiah (2014) Influence of lithium potassium zirconate nanoparticles on the electrical properties and structural characteristics of poly (vinylalcohol) films. *J Phys Chem Solids* 75:252–258. <https://doi.org/10.1016/j.jpics.2013.09.025>
2. Mo T-C, Wang H-W, Chen S-Y, Yeh Y-C (2008) Synthesis and dielectric properties of polyaniline/titanium dioxide nanocomposites. *Ceram Int* 34:1767–1771
3. Bekin S, Sarmad S, Gürkan K, Yenici G, Keçeli G, Gürdağ G (2014) Dielectric, thermal, and swelling properties of calcium ion-cross linked sodium alginate film. *Polym Eng Sci* 54:1372–1382
4. Vasudevan P, Thomas S, Arunkumar KV, Karthika S, Unnikrishnan NV (2015) Synthesis and dielectric studies of poly (vinyl pyrrolidone)/titanium dioxide nanocomposites. *IOP Conf Ser Mater Sci Eng* 73:012015. <https://doi.org/10.1088/1757-899x/73/1/012015>
5. Lucic Skoric M, Milosavljevic N, Radetic M, Saponjic Z, Radoicic M, Kalagasidis Krusic M (2015) Synthesis and characterization of interpenetrating polymer network based on sodium alginate and methacrylic acid and potential application for immobilization of TiO₂ nanoparticles. *Polym Eng Sci* 55:2511–2518
6. Rathna GVN, Birajdar MS, Bhagwani M, Paul VL (2013) Studies on fabrication, characterization, and metal extraction using metal chelating nonwoven nanofiber mats of poly (vinyl alcohol) and sodium alginate blends. *Polym Eng Sci* 53:321–333
7. Shi L, Xiong L, Hu Y, Li W, Chen ZC, Liu K, Zhang X (2017) Three-dimensional printing alginate/gelatin scaffolds as dermal substitutes for skin tissue engineering. *Polym Eng Sci*. <https://doi.org/10.1002/pen.24779>
8. Nawaz M, Moztahida M, Kim J, Shahzad A, Jang J, Miran W, Lee DS (2018) Photodegradation of microcystin-LR using graphene-TiO₂/sodium alginate aerogels. *Carbohydr Polym*. <https://doi.org/10.1016/j.carbpol.2018.07.007>
9. Thakur S, Sharma B, Verma A, Chaudhary J, Tamulevicius S, Thakur VK (2018) Recent progress in sodium alginate based sustainable hydrogels for environmental applications. *J Clean Prod*. <https://doi.org/10.1016/j.jclepro.2018.06.259>
10. Chen W, Feng Q, Zhang G, Yang Q, Zhang C (2017) The effect of sodium alginate on the flotation separation of scheelite from calcite and fluorite. *Miner Eng* 113:1–7
11. Yi X, Sun F, Han Z, Han F, He J, Minrui O, Junjie G, Xiaoping X (2018) Graphene oxide encapsulated polyvinyl alcohol/sodium alginate hydrogel microspheres for Cu (II) and U (VI) removal. *Ecotoxicol Environ Saf* 158:309–318
12. Wei S, Zhang X, Zhao K, Yifan F, Li Z, Lin B, Wei J (2016) Preparation, characterization and photocatalytic degradation properties of polyacrylamide/calcium alginate/TiO₂ composite film. *Polym Compos* 23:1292–1301

13. Wei S, Zhao K, Zhang X, Yifan F, Li Z, Wei J (2015) Adsorption and photocatalytic degradation of dyes on polyacrylamide/calcium alginate/TiO₂ composite film. *Funct Mater Lett* 8:1–5
14. Zhao K, Feng L, Lin H, Fu Y, Lin B, Cui W, Li S, Wei J (2014) Adsorption and photocatalytic degradation of methyl orange imprinted composite membranes using TiO₂/calcium alginate hydrogel as matrix. *Catal Today* 236:127–134
15. Zhao K, Feng L, Li Z, Yifan F, Zhang X, Wei J, Wei S (2014) Preparation, characterization and photocatalytic degradation properties of TiO₂/calcium alginate composite film and the recovery of TiO₂ nanoparticle. *RSC Adv* 4:51321–51329
16. Kothandan D, Kumar RJ, Prakash M, Naidu KCB (2018) Structural, morphological and optical properties of Ba_{1-x}Cu_xTiO₃ (x=0.2, 0.4, 0.6, 0.8) nanoparticles synthesized by hydrothermal method. *Mater Chem Phys* 215:310–315
17. Kumar NS, Suvarna RP, Naidu KCB, Kumar GR, Ramesh S (2018) Structural and functional properties of sol–gel synthesized and microwave heated Pb_{0.8}Co_{0.2-z}La_zTiO₃ (z=0.05–0.2) nanoparticles. *Ceram Int* 44:19408–19420
18. Kumar NS, Suvarna RP, Naidu KCB (2018) Sol–Gel synthesized and microwave heated Pb_{0.8-y}La_yCo_{0.2}TiO₃ (y=0.2–0.8) nanoparticles: structural, morphological and dielectric properties. *Ceram Int* 44:18189–18199
19. Sivakumar D, Naidu KCB, Nazeer KP, Rafi MM, Rameshkumar G, Sathyaseelan B, Killivalavan G, Begam AA (2018) Structural characterization and dielectric properties of superparamagnetic Iron oxide nanoparticles. *J Korean Ceram Soc* 55:230–238
20. Kumar DS, Naidu KCB, Rafi MM, Nazeer KP, Begam AA, Kumar GR (2018) Structural and dielectric properties of superparamagnetic iron oxide nanoparticles (SPIONs) stabilized by sugar solutions. *Mater Sci Pol* 36:123–133
21. Zangina T, Hassan J, Azis RS et al (2018) Structural, electrical conductivity and dielectric relaxation behavior of LiHf₂(PO₄)₃ ceramic powders. *J Aust Ceram Soc* 54:307–316
22. Naidu KCB, Reddy VN, Sarmash TS, Kothandan D, Subbarao T, Kumar NS (2018) Structural, morphological, electrical, impedance and ferroelectric properties of BaO–ZnO–TiO₂ ternary system. *J Aust Ceram Soc*. <https://doi.org/10.1007/s41779-018-0225-0>
23. Kumar NS, Suvarna RP, Naidu KCB (2019) Grain and grain boundary conduction mechanism in sol–gel synthesized and microwave heated PbLa_{0.8-y}Co_yTiO₃ (y=0.2–0.8) nanofibers. *Mater Chem Phys* 223:241–248
24. Hashim M, Raghasudha M, Shah J, Shirsath SE, Ravinder D, Kumar S, Meena SS, Bhatt P, Kumar R, Kotnala RK (2018) High temperature dielectric studies of indium-substituted NiCuZn nanoferrites. *J Phys Chem Solids* 112:29–36
25. Joshi S, Kumar M (2018) Effect of Ni²⁺ substitution on structural, magnetic, dielectric and optical properties of mixed spinel CoFe₂O₄ nanoparticles. *Ceram Int* 42:18154–18165
26. Naidu KCB, Madhuri W (2018) Ceramic nanoparticle synthesis at lower temperatures for LTCC and MMIC technology. *IEEE Trans Magn* 54:1–8. <https://doi.org/10.1109/tmag.2018.2855663>
27. Naidu KCB, Kumar NS, Kumar GR et al (2018) Temperature and frequency dependence of complex impedance parameters of microwave sintered NiMg ferrites. *J Aust Ceram Soc*. <https://doi.org/10.1007/s41779-018-0260-x>
28. Aravind G, Raghasudha M, Ravinder D, Vijaya Kumar R (2016) Magnetic and dielectric properties of Co doped nano crystalline Li ferrites by auto combustion method. *J Magn Magn Mater* 406:110–117